

Article

Influence of Ambient Humidity on the Performance of Complex Spectral Dielectric Films on SiO₂/K9 Substrates

Yizhang Ai ^{1,2}, Fang Wang ¹, Qilin Lv ², Hongjie Liu ^{1,*}, Yuan Chen ¹, Tianran Zheng ¹, Zairu Ma ² and Xuewei Deng ¹

¹ Research Center of Laser Fusion, China Academy of Engineering Physics, Mianyang 621900, China

² Department of Physics, School of Science, Xihua University, Chengdu 610039, China

* Correspondence: pandy_caep@163.com

Abstract: Ambient humidity is an important factor to consider when maintaining dielectric films' component performance. Herein, humidity-influenced experiments were conducted on complex spectral dielectric films based on SiO₂ and K9 substrates. Firstly, complex spectral dielectric films' spectral and surface stresses in different humidity environments were measured. Subsequently, laser-induced damage threshold measurements were carried out on these components. The experimental results indicate that the environmental humidity will induce the evolution of the internal structure of the dielectric films on the mirror, resulting in the deformation of the coating surface and a slight shift of the reflection spectrum. At the same time, the environmental humidity also greatly influences the anti-laser damage performance of the dielectric film mirror. Dielectric films based on SiO₂ have excellent damage resistance in high-humidity environments. Conversely, K9-based dielectric films have better damage resistance in low-humidity environments.

Keywords: ambient humidity; high-reflective mirror; dielectric films; laser-induced damage threshold



Citation: Ai, Y.; Wang, F.; Lv, Q.; Liu, H.; Chen, Y.; Zheng, T.; Ma, Z.; Deng, X. Influence of Ambient Humidity on the Performance of Complex Spectral Dielectric Films on SiO₂/K9 Substrates. *Crystals* **2023**, *13*, 248. <https://doi.org/10.3390/cryst13020248>

Academic Editor: Anna Paola Caricato

Received: 9 January 2023

Revised: 24 January 2023

Accepted: 29 January 2023

Published: 1 February 2023



Copyright: © 2023 by the authors. Licensee MDPI, Basel, Switzerland. This article is an open access article distributed under the terms and conditions of the Creative Commons Attribution (CC BY) license (<https://creativecommons.org/licenses/by/4.0/>).

1. Introduction

Laser inertial confinement fusion has been regarded as one of the key solutions to achieving controllable nuclear fusion [1–3]. In the past few decades, various large-scale laser facilities (e.g., National Ignition Facility [4], Laser Mega Joule [5]) have started to be successfully constructed for in-depth research on laser fusion. These high-power laser systems are so complex that thousands of optical components are adopted in the entire optical path arrangement, among which the number of reflection mirrors occupies the foremost place [6]. High-reflectivity mirrors are usually coated with optical films of different materials to meet specific requirements. The films have columnar microstructures [7,8], which can be easily invaded by moisture in storage and working environments and cause a series of problems: the thickness of the film evolution, which affects the performance of optical components [9]; the coefficient of expansion between the films are different, causing surface deformation and severe cracking of the film layer [10]; under the irradiation of the high-power laser, the coating is more susceptible to laser damage due to the intrusion of water molecules [11–14].

Meaningful research, both in theoretically and experimentally, has been dedicated to the influence of the ambient humidity of dielectric films. Stolz et al. [15] measured the spectra of electron-beam-deposited and ion-beam-assisted-deposited highly reflective films after switching from air to vacuum and found that the reduction in humidity caused spectral shifts of up to 3.5 percent. This experiment further helped other scholars to understand the performance for optimizing a vacuum operation and how to compensate for the coating design for a vacuum operation. Leplan et al. [16] studied the composition, density, and residual stress of SiO₂ films using the function of deposition parameters and aging behavior. For the first time, they tried to explain the long-term aging of SiO₂ films

and believed that the change of residual stress over time was water molecules reacting with encapsulated SiO₂ film pores with suspended silicon bonds. Anzellotti et al. [17] found the effect of ambient humidity on the stress and optical thickness of an HfO₂/SiO₂ polarizing film layer. They stored the film in air and dry nitrogen and pointed out that as the humidity decreased, the tensile stress of the film layer increased, and that the stress would exceed 30 MPa, resulting in an unqualified surface flatness. The optical thickness of the film decreases as the humidity decreases, and the degree of spectral shift is between 2% and 3%. Their study provided crucial insights into humidity-induced stress and optical thickness changes in hafnium/silica polarizing coatings.

Although these scholars have done valuable research, they have not compared the performance of dielectric film components based on different substrates under different humidity conditions, nor have they tested the laser anti-resistance damage performance of dielectric film components after changing the humidity environment. Meanwhile, there are few studies on the development of ambient humidity on complex spectral dielectric films on different substrates [15–18]. An in-depth understanding of the performance of complex spectral dielectric films on different substrates at different humidity levels is still in progress. Therefore, this study will delve into the effect of ambient humidity on the performance of complex spectral dielectric films on two usual substrates. It has significant implications for better understanding the effect of humidity on optical components, on how to store them and on how to maintain the operating performance of these devices.

2. Materials and Methods

2.1. Materials

Small-size complex spectral dielectric film samples (50 × 50 × 5 mm³) supplied by Oropt company were selected as experimental samples. It is a good choice to use small-size components to replace large-aperture optics, which can avoid damage to optical components during transportation and installation. Often used substrate materials are SiO₂ and K9, since they are available at a high quality at a reasonable cost and have a good optical quality for the visible range and somewhat into the infrared. Herein, SiO₂ and K9 glasses were chosen as the substrate materials for the experiment. A CeO₂ polishing agent was used to finely polish the substrate, so that the roughness R_q < 1 nm (measured with a roughness profiler). Subsequently, all the substrates were cleaned automatically on the cleaning line. First, the substrate is ultrasonically cleaned with a micro-90 cleaner, and then the substrate is rinsed with reverse osmosis (RO) water, and the above steps are repeated. After repeated cleaning, the deionized water generated in the circulation system is used to rinse the pure water. Finally, the substrate was taken out and subjected to infrared radiation drying. Substrates were coated with multilayer high-reflectivity dielectric films, which are alternative layers of hafnium oxide (HfO₂) and silicon dioxide (SiO₂) deposited by using electron beam evaporation [17–20]. The film system is designed according to Sub | (0.885H0.96L)¹⁵0.96L | Air, where “Sub” is substrate material, “H” is λ/4-thickness HfO₂, and “L” is λ/4-thickness SiO₂. The substrate parameters and the refractive index of the film material at different wavelengths [21] were listed in Tables 1 and 2, respectively.

Table 1. Substrate information for complex spectral dielectric membrane elements.

Substrate	Size	Quantity	Roughness	Processing Procedure
SiO ₂	50 × 50 × 5 mm ³	3	0.895/0.912/0.893	Fine polishing + cleaning + coating
K9	50 × 50 × 5 mm ³	3	0.912/0.913/0.875	Fine polishing + cleaning + coating

Table 2. Membrane material index for refraction at different wavelengths.

Material	HfO ₂						
	1064	1053	700	400	375	355	351
Refractive index	1.8810	1.8811	1.8902	1.9369	1.9490	1.9614	1.9642

Table 2. Cont.

Material	SiO ₂						
Lambda (nm)	1064	1053	700	400	375	355	351
Refractive index	1.4496	1.4498	1.4553	1.4701	1.4731	1.4761	1.4767

2.2. Laser-Induced Damage Threshold Measurements

Laser-induced damage experiments were performed on a small-diameter damage measurement platform to verify the influence of ambient humidity on the performance of dielectric membrane components. The layout of the working platform is shown in Figure 1. The output pulse from the Nd: YAG laser device has a wavelength of 1064 nm, a pulse width (FWHM) of 9 ns, and a diameter of 13 mm. The output energy of the laser is adjustable, the maximum output energy is 2 J, and the repetition frequency is adjustable from 1 Hz to 10 Hz. A 532 nm light output from a semiconductor laser facility is collimated for the Nd: YAG output pulse, so that the output pulse is precisely irradiated to the center of the sample area probed by a camera with a charged-coupled device (CCD camera). The beam-splitting wedge divides the output pulse into two paths. One path is the detection laser, which is received by the energy meter. On the other path, the laser passes through the optical wedge, condensed by the focusing lens ($f = 600$ mm) on the movable platform. An elliptical focusing spot with an area of about 2.43 mm^2 is obtained at a 45° angle on the sample surface. The damage-detection system observing the damage to the dielectric film consists of a CCD camera and a mobile control platform controlled by a computer. A Beam trap is applied to absorb the transmitted laser, which comes from the components in the system.

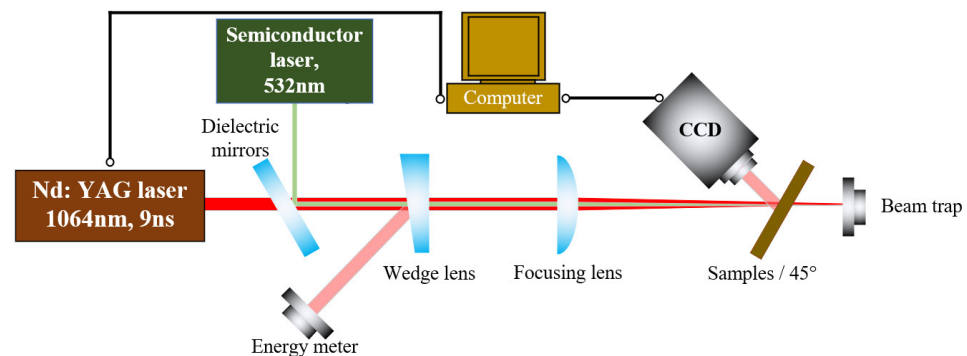


Figure 1. The layout of the working platform.

2.3. Introduction of Other Equipment

Water molecules in the air can enter the pore structure of the dielectric films and adsorb on its inner surface. Dipole interactions between water molecules on the inner surface of the pore structure of the dielectric film cause the film to expand or contract, causing water-induced stress, which changes the membrane's original stress distribution and surface shape. Therefore, we measured the stress of the dielectric films to study the effect of water molecules in the air on the coatings. We chose to measure the shape of the reflective surface of the dielectric films under different ambient humidity values to characterize the change of film stress. The principle of this method is that coating stress affects the flatness of the coating, which in turn causes wavefront distortion of the incident beam reflected by the optical element. The reflected wavefront measurements were performed on a Zygo Mark-GPI interferometer. In addition, a spectrophotometer (Lambda 950 UV/Vis/NIR) was applied to characterize the spectral information of the samples.

After the preparation of the experimental equipment was completed, the experimental process was as follows: three samples of each kind of substrate were stored in a 25% humidity environment for four weeks. After storage, three samples were taken out for

reflected wavefront testing and spectral testing, and one was taken out for laser damage testing. Subsequently, the remaining two samples were stored at 50% humidity for four weeks. After storage, the two samples were taken out for reflected wavefront testing and spectral testing, and one was taken out for laser damage testing. Finally, the remaining piece sample was stored in an environment with 70% humidity for four weeks. After storage, reflected-wavefront, spectrum, and laser-damage tests were performed. All the storage environmental humidity of the experimental optical components was tested with a hygrometer at a temperature of 21 degrees Celsius.

3. Discussions

3.1. Influence of Ambient Humidity on the Surface Shape of the Complex Spectral Dielectric Films

Figure 2 illustrates the reflector shape and gradient data (de-slope processing) for dielectric films at different ambient humidity values. As shown in Figure 2a, the Peak-to-Valley (PV) value of the SiO₂-based dielectric films under the 25% humidity environment is $\sim 0.228\lambda$, and the RMS value is $\sim 0.0639\lambda$. With the increase in storage humidity, the PV value of the dielectric films decreased by $\sim 2.63\%$ and $\sim 2.63\%$, respectively. In Figure 2b, the PV value of the K9-based dielectric films under the 25% humidity environment is $\sim 0.457\lambda$, and the RMS value is $\sim 0.0690\lambda$. With the increase in the humidity environment, the PV value of the dielectric films decreased by $\sim 50.5\%$ and $\sim 45.3\%$; the RMS value decreased by $\sim 40.4\%$ and $\sim 53.6\%$, respectively. One can see that the stress of the dielectric films is sensitive to humidity, and the dielectric films based on K9 are more seriously affected by water molecules. The reason for this phenomenon is hydration: SiO₂ chemically reacts with water molecules to generate various forms of silicic acid, and the lattice shrinkage of SiO₂ shrinks the film, thereby generating tensile stress and releasing the original compressive stress. At the same time, the Silicon-alcohol-based (HO-Si-OH) groups in the silicic acid generated by hydration generate a permanent electric dipole moment [8,10,22], and the electrostatic interaction between the dipoles generates tensile stress. As a result, the compressive stress of the film is gradually reduced and transformed into tensile stress, resulting in a depression on the coatings' surface. What needs to be illustrated is that although the K9-based dielectric film does not change so regularly under different humidity environments, the surface shape still has a concave trend as the humidity increases. This phenomenon may be because the combined stress between the film layer and the substrate is slowly released over time [23]. This particularity arises because the stress change caused by the subsequent humidity change is small, while the original large stress release effect is reflected. Compared with the dielectric film on the SiO₂ substrate, the dielectric film on the K9 substrate is more sensitive to ambient humidity.

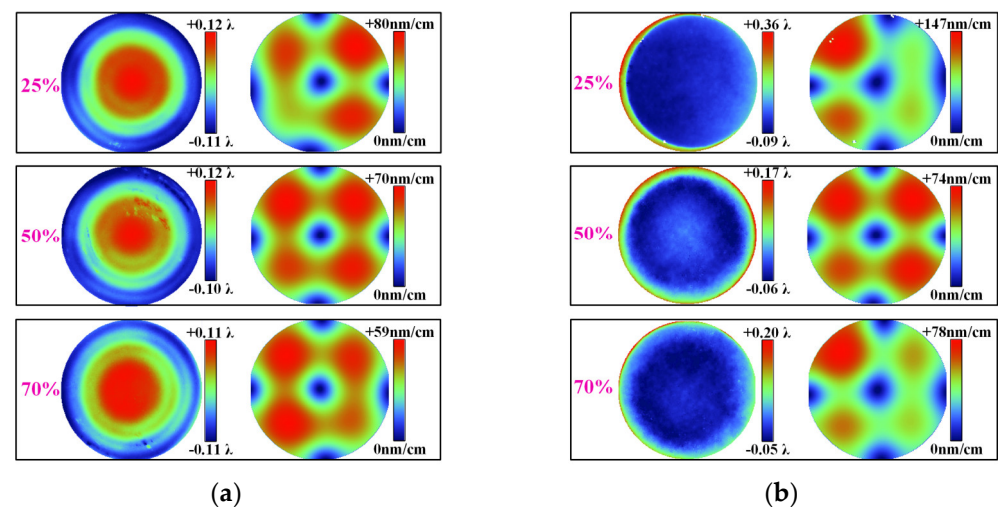


Figure 2. The reflective surface shape and gradient data (de-slope processing) for dielectric films at 25%, 50%, and 70% ambient humidity. (a) SiO₂-substrate dielectric films; (b) K9-substrate dielectric films.

3.2. Influence of Ambient Humidity on Reflective Properties of the Complex Spectral Dielectric Films

The requirements for the average spectral response of the complex spectral dielectric films' mirror are the following spectral reflectivity: $R(351\text{ nm}) < 33\%$; $R(375\text{ nm}) > 97\%$; $R(400\text{--}700\text{ nm}) < 33\%$; and $R(1064\text{ nm}) > 99.5\%$ [19,20]. As shown in Figure 3, at a 50% ambient humidity (initial humidity environment for sample storage), the reflectivity values of the dielectric films' sample on the SiO_2 substrate and the dielectric films' sample on the K9 substrate at 1064 nm are 99.58% and 99.52%, respectively; at 375 nm, the reflectivity values are 98.51% and 99.53%, respectively; at 351 nm, the reflectivity values are 10.26% and 15.55%, respectively; at 400 nm~700 nm, the reflectivity is less than 30.51%. The reflectivities at the abovementioned wavelengths' positions meet the reflect mirror design and experimental requirements.

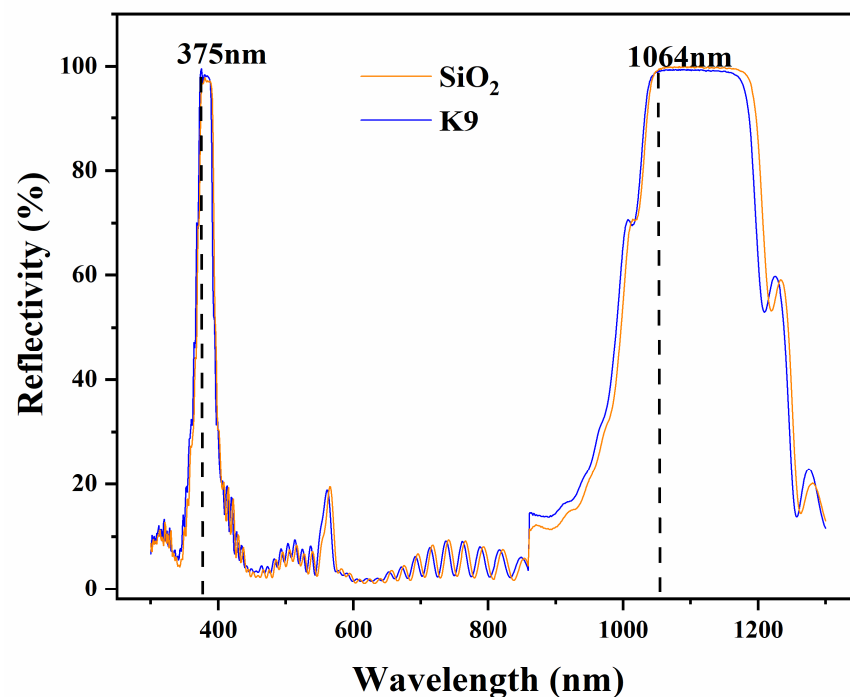


Figure 3. The spectra of high-reflectivity dielectric coatings based on SiO_2 and K9 (in a 50% humidity environment).

After the experimental samples were stored for four weeks, we carried out reflectance measurements on these samples. Figure 4 shows the reflectance spectra of the samples stored at different ambient humidity values. In a 25% humidity environment, the original spectral peak of SiO_2 -based dielectric film components at 1064 nm shifted to 1048 nm, moving by $\sim 1.5\%$; the initial spectral peak at 351 nm moved to 343 nm, moving by $\sim 2.3\%$. In a 50% humidity environment, the spectrum showed almost no shift. In a 70% humidity environment, the original spectral peak at 1064 nm shifted to 1077 nm, shifting by $\sim 1.2\%$; the spectral peak at 351 nm shifted to 352 nm, shifting by $\sim 0.3\%$. One can see that the spectrum position of SiO_2 -based dielectric films shifted to the long spectrum with an increase in humidity. For the dielectric film based on K9, under 25% humidity, the original spectral peak at 1064 nm shifted to 1060 nm, moving by $\sim 0.4\%$; the initial spectral peak at 351 nm hardly shifted. In a 50% humidity environment, the spectrum's peak did not shift significantly. In a 70% humidity environment, the original spectral peak at 1064 nm moved to 1046 nm, shifting by $\sim 1.7\%$; the peak at 351 nm moved to 350 nm, shifting by $\sim 0.3\%$. Compared with the initial K9-based dielectric films' spectrum, the spectrum shifted toward the short-spectrum direction, in both the 70% ambient humidity environment and the 25% ambient humidity environment. The reflectivity at different wavelengths of samples

stored for four weeks in different humidity environments is given in Figure 5. Although the refractive index at different wavelengths was changed, it can still meet the design requirements of optical components.

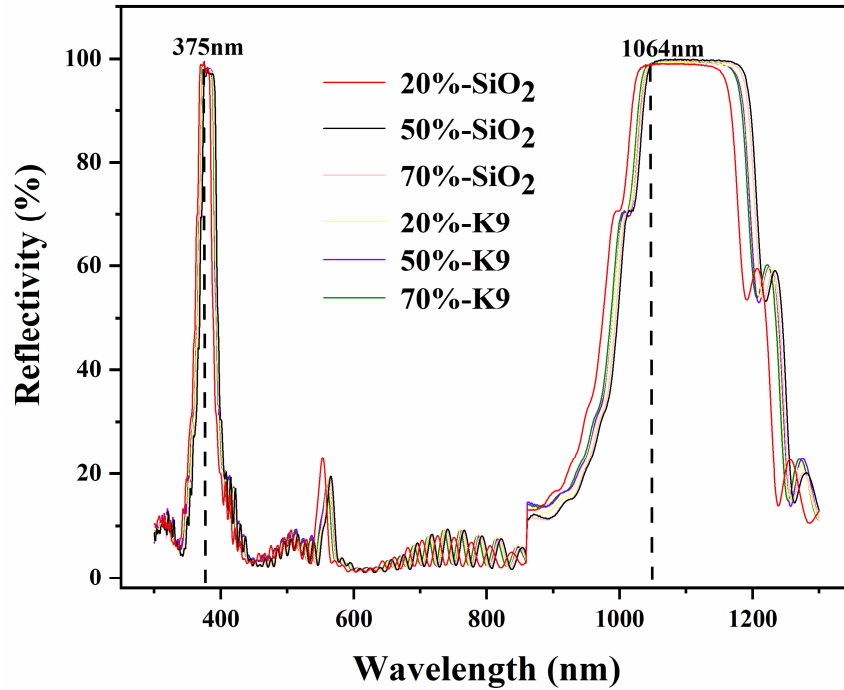


Figure 4. The spectra of high-reflectivity dielectric coatings based on SiO₂ and K9 in different humidity environments.

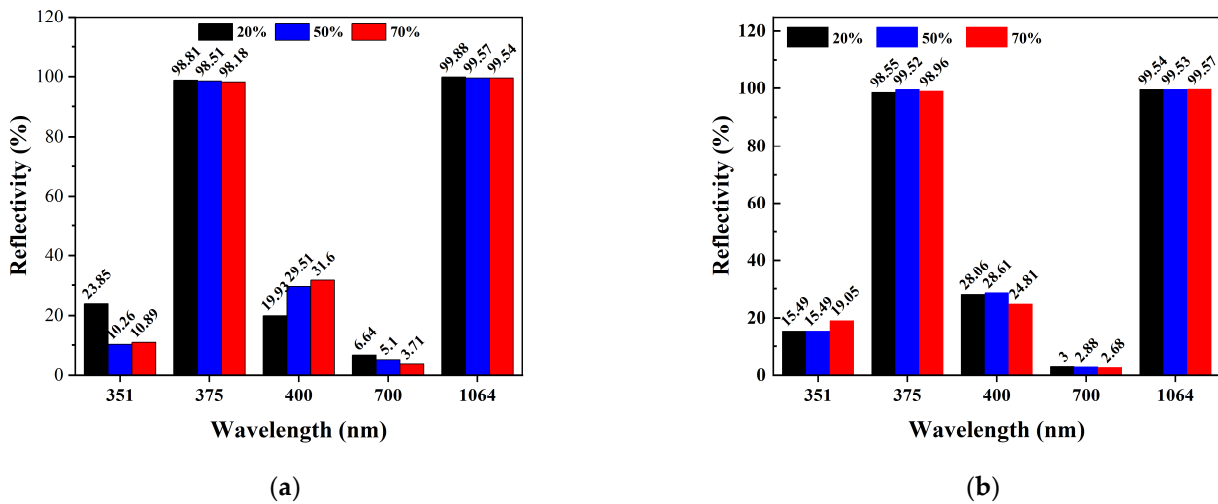


Figure 5. The reflectivity at 351 nm, 375 nm, 400 nm, 700 nm, and 1064 nm wavelengths of samples stored for four weeks in different humidity environments: (a) SiO₂ and (b) K9.

The adsorption of moisture leads to a certain shift in the spectrum of the optical films (the immersion of water molecules in the film changes the thickness of the film, thereby changing the reflectivity), which is the main reason for the optical performance instability of coatings. Due to the different refractive indices of water and air, thin film pores with a low water content have a low optical thickness, resulting in a shift in spectral reflectance or transmittance to shorter wavelengths. Conversely, film pores with a high water content have a high optical thickness, and the reflectance or transmittance of the spectrum shifts to

longer wavelengths. Regarding the phenomenon of an irregular spectral drift, this may be caused by the uneven electron-beam-deposition and ion-beam-assisted-deposition process.

3.3. Laser-Induced Damage Threshold Results

To illustrate the influence of ambient humidity on the laser-induced damage of dielectric films component, we adopted R-on-1 to obtain the damage threshold of the component. The laser-induced damage threshold is measured strictly according to the specifications required by the international standard ISO21254. Figure 6 shows the measurement results of the damage probability: Figure 6a plots the damage probability curve of the SiO₂ substrate samples under different ambient humidity values, and Figure 6b shows the damage probability curve of the K9 substrate samples under different ambient humidity values. From Figure 6a, as the output laser fluence increases, the laser damage threshold of dielectric films in the 70% humidity environment is ~24 J/cm². In the 50% humidity environment, it is ~17 J/cm². In the 25% humidity environment, it is ~14 J/cm². Under the maximum laser fluence that the laser can output, the damage probability of the SiO₂-based dielectric film sample in the 25% humidity environment is approximately five times above that in the 70% humidity environment. Figure 6b shows that the laser damage threshold of the K9-based dielectric films under a 70% humidity environment is ~11 J/cm². In the 50% humidity environment, it is ~20.5 J/cm². In the 25% humidity environment, it is ~23.7 J/cm². Under the maximum laser fluence that the laser can output, the damage probability of the K9-based dielectric film sample in a 70% humidity environment is about 1.4 times that in a 25% humidity environment.

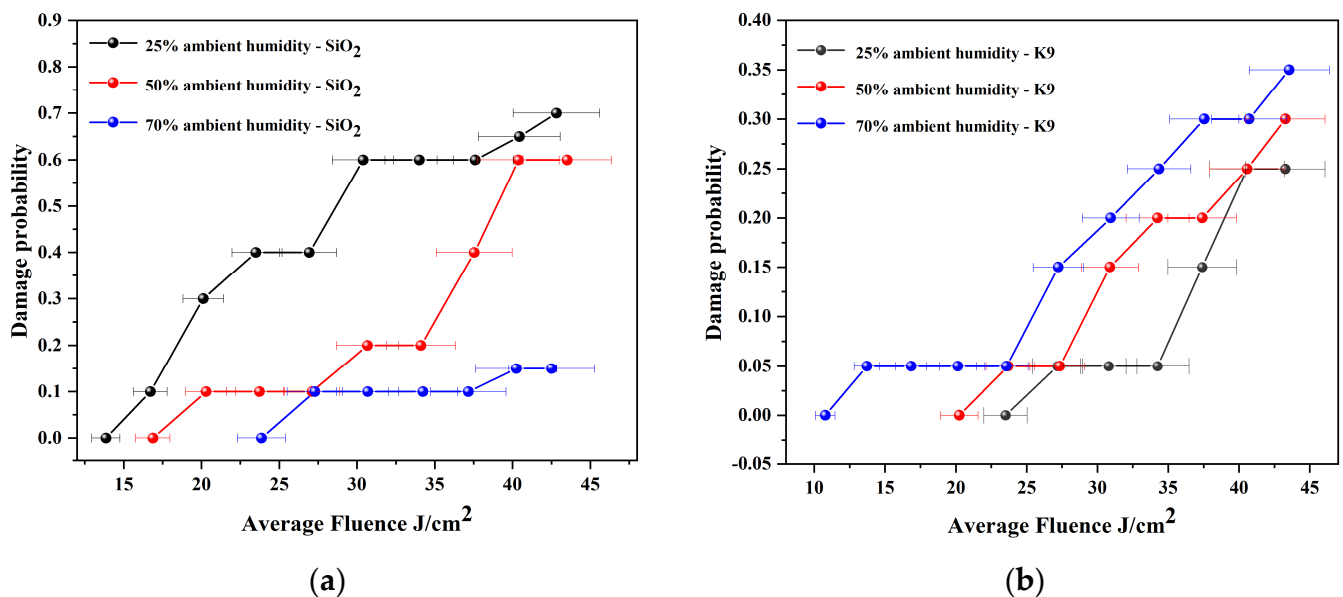


Figure 6. Damage probability: (a) SiO₂ substrate dielectric films; (b) K9 substrate dielectric films, 6.5% errors.

From the experimental results, it can be seen that the environmental humidity will inevitably influence the damage resistance of the dielectric films. The dielectric films based on SiO₂ have a better damage resistance in a high-humidity environment. In comparison, the dielectric films based on K9 have a better damage resistance in a low-humidity environment. Different substrate materials had various physical and chemical properties when the films were combined with the substrate, which affected the film-substrate adhesion and mechanical strength, and then significantly influenced the laser resistance of the entire film-substrate combination. The influencing factors may include the following:

- (1) The surface roughness will directly affect the film surface roughness of the deposited films, affecting the anti-laser damage ability of optical components [24];

- (2) The geometric, physical, and chemical structures of the substrate surface and adjacent regions change the shape and properties of the interfacial layer, which is related to the choice of substrate material and the processing and cleaning of the substrate [8,14]. The substrate surface preprocessing, such as cutting and polishing, changes the surface geometry, mechanical structure, and the surface's chemical structure. The polished glass substrate forms a layer of polishing material on its surface, such as a mixture of oxides, reaction products, water, and glass particles. A cleaning treatment after polishing is very important [12];
- (3) The influence of material parameters on the substrate's self-weight and thermal deformation: The difference in density and elastic modulus determines the difference in the substrates' self-weight deformation, and the difference in their linear thermal expansion coefficient also leads to a difference in their thermal deformation [25];
- (4) The substrate will be deformed by weight under the fixture's support during the vacuum coating process. At the same time, during the electron beam evaporation coating, the inevitable temperature inhomogeneity during baking will cause a certain temperature gradient distribution inside the substrate, resulting in thermal stress deformation of the substrate. During the coating process, the prestress of the substrate will have a stress coupling effect with the stress of the film, thus affecting the surface shape of the film-substrate system [26].

4. Conclusions

In this work, the evolutions, in terms of the reflection spectrum, surface shape and laser damage threshold, of complex spectral dielectric films based on SiO₂ and K9 were measured under different ambient humidity values. The experimental results demonstrate that the stress of the complex spectral dielectric films is sensitive to humidity and that the intrusion of water molecules can cause the surface shape of the dielectric film element to be deformed, thereby influencing the performance of the mirror. At the same time, the change in ambient humidity can cause a slight shift in the reflection spectrum. The spectrum position of SiO₂-based dielectric films shifts to the long spectrum with an increase in humidity. The K9-based dielectric films' spectrum shifts toward the short-spectrum direction when compared to the 50% ambient humidity, in both the 70% ambient humidity environment and 25% ambient humidity environment. Compared with the dielectric films based on SiO₂, the surface shape of dielectric films based on K9 is severely affected by the impact of water molecules. Dielectric films based on SiO₂ have a better laser damage resistance in high-humidity environments. On the contrary, the K9-based dielectric films have a better laser damage resistance in low-humidity environments. This work provides a reference value for selecting high-reflecting mirror substrate materials. Furthermore, this work also provides guidance for the storage of high-reflectivity dielectric film components.

Author Contributions: Conceptualization, F.W. and H.L.; methodology, F.W. and H.L.; validation, F.W. and H.L.; analysis, Y.A. and F.W., and H.L. and Q.L.; investigation, Y.A. and Q.L.; data curation, Y.C. and T.Z.; writing—original draft preparation, Y.A.; writing—review and editing, Y.A. and F.W., and H.L. and Z.M.; supervision, F.W., and H.L. and X.D.; project administration, F.W., and H.L. and X.D. All authors have read and agreed to the published version of the manuscript.

Funding: The authors are grateful for the support of the National Natural Science Foundation of China CNSTC (62175222, 62005258).

Data Availability Statement: The data that support the findings of this study are available from the corresponding author upon reasonable request.

Acknowledgments: The authors acknowledge support from the Institute of Research Center of Laser Fusion.

Conflicts of Interest: The authors declare no conflict of interest.

References

1. Spaeth, M.L.; Manes, K.R.; Kalantar, D.H.; Miller, P.E.; Heebner, J.E.; Bliss, E.S.; Spec, D.R.; Parham, T.G.; Whitman, P.K.; Wegner, P.J.; et al. Description of the NIF Laser. *Fusion Sci. Technol.* **2016**, *69*, 25–145. [[CrossRef](#)]
2. Betti, R.; Hurricane, O.A. Inertial-confinement fusion with lasers. *Nat. Phys.* **2016**, *12*, 435–448. [[CrossRef](#)]
3. Kline, J.; Batha, S.; Benedetti, L.; Bennett, D.; Bhandarkar, S.; Hopkins, L.B.; Biener, J.; Biener, M.; Bionta, R.; Bond, E.; et al. Progress of indirect drive inertial confinement fusion in the United States. *Nucl. Fusion* **2019**, *59*, 112018. [[CrossRef](#)]
4. Spaeth, M.L.; Manes, K.R.; Bowers, M.; Celliers, P.; Di Nicola, J.-M.; Di Nicola, P.; Dixit, S.; Erbert, G.; Heebner, J.; Kalantar, D.; et al. National Ignition Facility Laser System Performance. *Fusion Sci. Technol.* **2016**, *69*, 366–394. [[CrossRef](#)]
5. Miquel, J.L.; Batani, D.; Blanchot, N. Overview of the laser mega joule (LMJ) facility and PETAL project in France. *Rev. Laser Eng.* **2014**, *42*, 131–136. [[CrossRef](#)] [[PubMed](#)]
6. Baisden, P.A.; Atherton, L.J.; Hawley, R.A.; Land, T.A.; Menapace, J.A.; Miller, P.E.; Runkel, M.J.; Spaeth, M.L.; Stolz, C.J.; Suratwala, T.I.; et al. Large Optics for the National Ignition Facility. *Fusion Sci. Technol.* **2016**, *69*, 295–351. [[CrossRef](#)]
7. Field, E.S.; Bellum, J.C.; Kletecka, D.E. How reduced vacuum pumping capability in a coating chamber affects the laser damage resistance of HfO₂/SiO₂ antireflection and high-reflection coatings. *Opt. Eng.* **2016**, *56*, 011005. [[CrossRef](#)]
8. Li, Y.; Bai, Q.; Yao, C.; Zhang, P.; Shen, R.; Liu, H.; Lu, L.; Jiang, Y.; Yuan, X.; Miao, X.; et al. Long-lasting antifogging mechanism for large-aperture optical surface in low-pressure air plasma in-situ treated. *Appl. Surf. Sci.* **2022**, *581*, 152358. [[CrossRef](#)]
9. Hossain, M.F.; Pervez, M.S.; Nahid, M.A.I. Influence of film thickness on optical and morphological properties of TiO₂ thin films. *Emerg. Mater. Res.* **2020**, *9*, 186–191. [[CrossRef](#)]
10. Zhu, P.; Shen, W.X.; Chen, W.H.; Zhang, W. Aging and humidity effects of optical surface deformation after deposition. *High Power Laser Part. Beams* **2009**, *21*, 851–854.
11. Liu, Z.; Luo, J.; Zheng, Y.; Ma, P.; Zhang, Z.; Wei, Y.; Pan, F.; Chen, S. Damage morphology change condition and thermal accumulation effect on high-reflection coatings at 1064nm. *Opt. Express* **2014**, *22*, 10151–10164. [[CrossRef](#)] [[PubMed](#)]
12. Yin, J.; Cao, Y. Research of laser-induced damage of aluminum alloy 5083 on micro-arc oxidation and composite coatings treatment. *Opt. Express* **2019**, *27*, 18232–18245. [[CrossRef](#)] [[PubMed](#)]
13. Peng, G.; Chen, J.; Lu, L.; Miao, X.; Dong, Z.; Leng, D. Dual dynamic airflow protection for the removal of fused silica micron particles in the final optics assembly. *Aerosol Sci. Technol.* **2020**, *54*, 342–352. [[CrossRef](#)]
14. Li, Y.; Bai, Q.; Guan, Y.; Zhang, P.; Shen, R.; Lu, L.; Liu, H.; Yuan, X.; Miao, X.; Han, W.; et al. In situ plasma cleaning of large-aperture optical components in ICF. *Nucl. Fusion* **2022**, *62*, 076023. [[CrossRef](#)]
15. Stolz, C.J.; Taylor, J.R.; Eickelberg, W.K.; Lindh, J.D. Effects of vacuum exposure on stress and spectral shift of high reflective coatings. *Appl. Opt.* **1993**, *32*, 5666–5672. [[CrossRef](#)] [[PubMed](#)]
16. Leplan, H.; Geenen, B.; Robic, J.Y.; Pauleau, Y. Residual stresses in evaporated silicon dioxide thin films: Correlation with deposition parameters and aging behavior. *J. Appl. Phys.* **1995**, *78*, 962–968. [[CrossRef](#)]
17. Anzellotti, J.F.; Smith, D.J.; Sczupak, R.J.; Chrzan, Z.R. Stress and environmental shift characteristics of HfO₂/SiO₂ multilayer coatings. In Proceedings of the Laser-Induced Damage in Optical Materials: 1996, Boulder, CO, USA, 13 May 1997.
18. Jena, S.; Tokas, R.; Thakur, S.; Udupa, D. Study of aging effects on optical properties and residual stress of HfO₂ thin film. *Optik* **2019**, *185*, 71–81. [[CrossRef](#)]
19. Stolz, C.J.; Weinzapfel, C.L.; Rigatti, A.L.; Oliver, J.B.; Taniguchi, J.; Bevis, R.P.; Rajasansi, J.S. Fabrication of meter-scale laser resistant mirrors for the National Ignition Facility: A fusion laser. In Proceedings of the Advances in Mirror Technology for X-Ray, EUV Lithography, Laser, and Other Applications, San Diego, CA, USA, 13 January 2004.
20. Stolz, C.J.; Miller, P.E.; Cross, D.A.; Davis, J.A.; Sommer, S.C.; Widmayer, C.C.; MacGowan, B.J.; Whitman, P.K.; Qiu, S.R.; Negres, R.A.; et al. Transport mirror laser damage mitigation technologies on the National Ignition Facility. In Proceedings of the Advances in Optical Thin Films VI, Frankfurt, Germany, 5 June 2018.
21. Refractive Index. INFO Website. Available online: <https://refractiveindex.info/> (accessed on 11 October 2022).
22. Leplan, H.; Robic, J.Y.; Pauleau, Y. Kinetics of residual stress evolution in evaporated silicon dioxide films exposed to room air. *J. Appl. Phys.* **1996**, *79*, 6926–6931. [[CrossRef](#)]
23. Abadias, G.; Chason, E.; Keckes, J.; Sebastiani, M.; Thompson, G.B.; Barthel, E.; Doll, G.L.; Murray, C.E.; Stoessel, C.H.; Martinu, L. Review Article: Stress in thin films and coatings: Current status, challenges, and prospects. *J. Vac. Sci. Technol. A Vac. Surf. Film.* **2018**, *36*, 020801. [[CrossRef](#)]
24. Deng, W.H. Study on the Influence of 1064nm/532nm Lasers on the Damage Threshold of Thin Films. Master's Thesis, Xi'an Technological University, Xi'an, China, 2022.
25. Zhu, P.; Zhu, J.Q. Influences of the Substrate Stress on Element Surface Figure. *Chin. J. Lasers* **2009**, *36*, 4.
26. Li, Y. Preparation and Deformation Analysis of 1064nm Reflective Films for High Energy Laser Systems. Master's Thesis, Xi'an Technological University, Xi'an, China, 2021.

Disclaimer/Publisher's Note: The statements, opinions and data contained in all publications are solely those of the individual author(s) and contributor(s) and not of MDPI and/or the editor(s). MDPI and/or the editor(s) disclaim responsibility for any injury to people or property resulting from any ideas, methods, instructions or products referred to in the content.